Nuclear Instruments and Methods in Physics Research A 1057 (2023) 168795

Contents lists available at ScienceDirect

Nuclear Inst. and Methods in Physics Research, A

journal homepage: www.elsevier.com/locate/nima

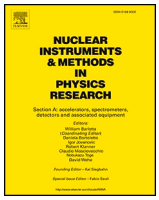

Calibration of the NEVOD-EAS array for detection of extensive air showers

M.B. Amelchakov [a], A.G. Bogdanov [a], A. Chiavassa [b,c,*], A.N. Dmitrieva [a], D.M. Gromushkin [a], E.P. Khomchuk [a], S.S. Khokhlov [a], R.P. Kokoulin [a], K.G. Kompaniets [a], A. Yu Konovalova [a], G. Mannocchi [d], K.R. Nugaeva [a], A.A. Petrukhin [a], I.A. Shulzhenko [a], G. Trinchero [c,d], I.I. Yashin [a], E.A. Yuzhakova [a]

[a] National Research Nuclear University MEPhI (Moscow Engineering Physics Institute), 115409, Moscow, Russia
[b] Dipartimento di Fisica dell' Università degli Studi di Torino, 10125, Torino, Italy
[c] Sezione di Torino dell' Istituto Nazionale di Fisica Nucleare – INFN, 10125, Torino, Italy
[d] Osservatorio Astrofisico di Torino – INAF, 10025, Torino, Italy

ARTICLE INFO

Keywords:
Extensive air showers
Detectors calibration
NEVOD-EAS
URAGAN
DECOR
Experimental complex NEVOD

ABSTRACT

In this paper we discuss the calibration of the NEVOD-EAS array which is a part of the Experimental Complex NEVOD, as well as the results of studying the response features of its scintillation detectors. We present the results of the detectors energy calibration, performed by comparing their response to different types of particles obtained experimentally and simulated with the Geant4 software package, as well as of the measurements of their timing resolution. We also discuss the results of studies of the light collection non-uniformity of the NEVOD-EAS detectors and of the accuracy of air-shower arrival direction reconstruction, which have been performed using other facilities of the Experimental Complex NEVOD: the muon hodoscope URAGAN and the muon tracking detector DECOR.

1. Introduction

Detection of extensive air showers (EAS) is the only way to study primary cosmic rays with energies above 10^{15} eV. In most experiments measuring extensive air showers, the reconstruction of the primary particle characteristics is based on the analysis of the energy deposit of shower particles in an array of detectors. Most of the energy deposited is due to the interaction of air-shower electromagnetic component with the detector material. Air-shower parameters are estimated by approximating the energy deposits observed in the array of detectors with the lateral distribution function of EAS electrons [1]. So, an important aspect of the experiment is the detector energy calibration, i.e. the determination of the detector response to energy released by EAS particles.

The energy calibration is performed by comparing the amplitude or charge spectra of detector responses with those obtained by calculations or simulation, as done in the EAS-TOP [2], KASCADE [3], KASCADE-Grande [4], Pierre Auger [5], Tibet air-shower array [6], Ice-Top [7], LHAASO [8], etc.

When an air-shower array is operated together with other facilities, it becomes possible to carry out various cross-calibrations. For instance, the EAS parameters reconstructed by Cherenkov water detectors and using the fluorescence method were compared at the Pierre Auger Observatory [9]; the characteristics of EASs recorded simultaneously in the KASCADE and KASCADE-Grande arrays [4] were compared; the air-shower events in the Tunka-133 experiment were used to calibrate the radio method [10]; the IceTop array was used to check the accuracy of muon bundle arrival direction reconstruction in the IceCube detector [11].

The Experimental Complex NEVOD [12] is located in the campus of the National Research Nuclear University MEPhI (Moscow, Russia) and is designed to study all components of cosmic rays with primary energies in the range from 10^{10} to 10^{19} eV. Initially, the complex included the Cherenkov water detector NEVOD with a volume of 2000 m^3 surrounded by the muon tracking detector DECOR. With the NEVOD and DECOR detectors we measured extensive air showers arriving at zenith angles larger than 55°. In this case, only EAS muon component, which is detected as muon bundles, reaches the facilities. Based on the multiplicity of muons in a bundle and its arrival direction zenith angle, we estimated the primary particle energy. By comparing the results of

* Corresponding author. Dipartimento di Fisica dell' Università degli Studi di Torino, 10125, Torino, Italy.
E-mail address: andrea.chiavassa@unito.it (A. Chiavassa).

https://doi.org/10.1016/j.nima.2023.168795
Received 23 June 2023; Received in revised form 12 September 2023; Accepted 14 October 2023
Available online 16 October 2023

experiment and simulation the excess of muons (so-called "muon puzzle"), was discovered [13]. Later this result was confirmed in other experiments [14]. Obviously, these results depend on models of hadronic interaction used in simulation. To validate such approach, a dedicated NEVOD-EAS array measuring electron-photon component of air-showers was constructed. Simultaneous measuring of the same air-shower by two independent facilities detecting EAS electron-photon and muon components, NEVOD-EAS and DECOR, will provide the opportunity to compare primary particle energies evaluated from the data of both experiments. In addition, the PRISMA and URAN arrays for detecting EAS hadronic component by means of thermal neutrons were constructed at the Experimental Complex NEVOD.

In this paper we discuss the calibration of the NEVOD-EAS array, as well as the results of a detailed study of the performance of the scintillation detectors used.

2. The NEVOD-EAS air-shower array

The NEVOD-EAS array [15] is designed to detect the electron-photon component of extensive air showers with energies in the range from 10^{15} to 10^{17} eV. It includes 36 scintillation detector stations (DSs) deployed over an area of about 10^4 m^2 on the roofs of laboratory buildings of the Experimental Complex NEVOD and on the ground surface. Stations are combined into 9 clusters. The layout of the DSs and clusters of the array is shown in Fig. 1.

Each cluster consists of 4 DSs (Fig. 2) located at the vertices of a quadrilateral (mainly a rectangle) with typical side lengths of about 15 m, as well as of a local post for preliminary data processing. The cluster local post receives and digitizes analog signals from detector stations, selects events according to intra-cluster trigger conditions, assigns timestamps to events, and, thus, operates as an independent air-shower installation measuring both the number of particles detected by each DS and the EAS arrival direction.

The main elements of the NEVOD-EAS array are scintillation detectors sensitive to charged particles, mainly electrons, of extensive air showers (Fig. 2, right). These detectors were previously used in the EAS-TOP [16] and KASCADE-Grande [4] experiments. The NEVOD-EAS detectors [17] consist of a plastic scintillator NE102A [19] with dimensions of 800 × 800 × 40 mm^3 and one or two (see below)

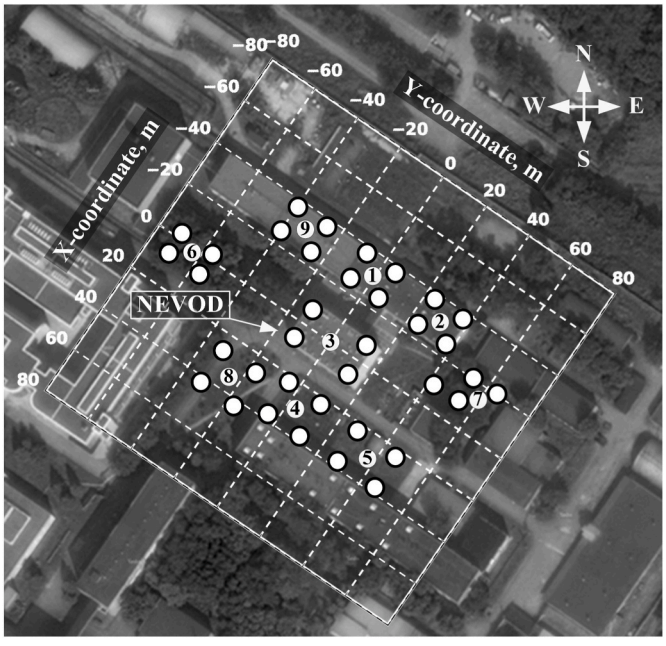

Fig. 1. The layout of the detector stations and clusters of the NEVOD-EAS array [15].

photomultipliers (PMTs) Philips XP3462 [21]. The scintillator and PMTs are enclosed inside a light-insulated stainless steel pyramidal housing. To improve light collection, the inner surface of the housing is painted with a diffusely reflective coating. The distance between the PMT photocathode and the scintillator is 300 mm.

Each detector station consists of four scintillation detectors installed inside a protective external housing (Fig. 2, top left) and has an area of 2.56 m^2. Three detectors of the station are equipped with one PMT operating at high gain (in the following named "standard"). The fourth detector includes two PMTs: the standard photomultiplier and an additional one working at a lower gain. Standard PMTs are used to measure the EAS particle densities of up to ~100 particles/m^2 and for time measurements. The additional PMT expands the DS dynamic range up to ~10^4 particles/m^2 when detecting EASs with high particle density.

3. Simulation of the NEVOD-EAS detector and detector station

To perform the energy calibration of the NEVOD-EAS detector station, we have developed the models of the scintillation detector and DS using the Geant4 software package [18]. The models take into account the geometry of the detector and DS, as well as physical and chemical properties of materials and surfaces.

The detector geometry includes the following main elements: a metal housing, a scintillation plate, two scintillator's supports (see Fig. 2, right), glass and a photocathode of PMT.

Sheet steel with thickness of 1 mm is used as the housing material. The reflection coefficient, of the coating used to paint the inner surface of detector housing, is 0.9. This value was selected by iterative comparison of experimental and simulated matrices of the normalized charge of the NEVOD-EAS detector responses (see Section 4).

The NE102A scintillator [19] has the following properties: a density of 1.032 g/cm^3, a light refractive index of 1.58, a light yield of 12000 photons/MeV, an emission time of 2.4 ns, and a light absorption length of 1 m. The dependence of the scintillator relative light yield on the energy of emitted photons, which we embedded in the model, is shown in Fig. 3 (curve No. 2).

The scintillator's supports have the shape of parallelepipeds and consist of PMMA [20] with a density of 1.19 g/cm^3 and a refractive index of 1.49. Since the supports are small, the impact of light attenuation length was neglected in the simulation by setting a relatively large value (5 m).

The input window of the PMT [21] is a cylinder with a diameter of 76 mm and a height of 13 mm. The material of the input window is glass with a density of 2.53 g/cm^3, a refractive index of 1.54, and a light attenuation length of 5 m. The hemispherical PMT photocathode is set as a metal surface.

The probability of photoelectron emission was simulated using the dependence of the photomultiplier quantum efficiency on the photon energy, which is shown in Fig. 3 (curve No. 1). The charge of a pulse at the PMT output was modeled as the sum of PMT responses to single photoelectrons. The charge of PMT response to each photoelectron was drawn according to the normal distribution. The parameters of this distribution were determined using a typical charge spectrum of the PMT Philips XP3462 responses to single photoelectron illumination, which was measured at a gain of 2×10^6 (Fig. 4). The average charge of single-electron signals is 0.31 ± 0.01 pC, and the FWHM of the distribution is ~0.3 pC.

The model of the detector station includes an array of four identical scintillation detectors placed inside an external housing made of sheet steel with a thickness of 0.7 mm. When simulating the passage of particles, the response of the detector station is the sum of the responses of 4 scintillation detectors included in it, as it is done in experiment [15].

4. Verification of the detector model

To verify the model of the scintillation detector, we have compared

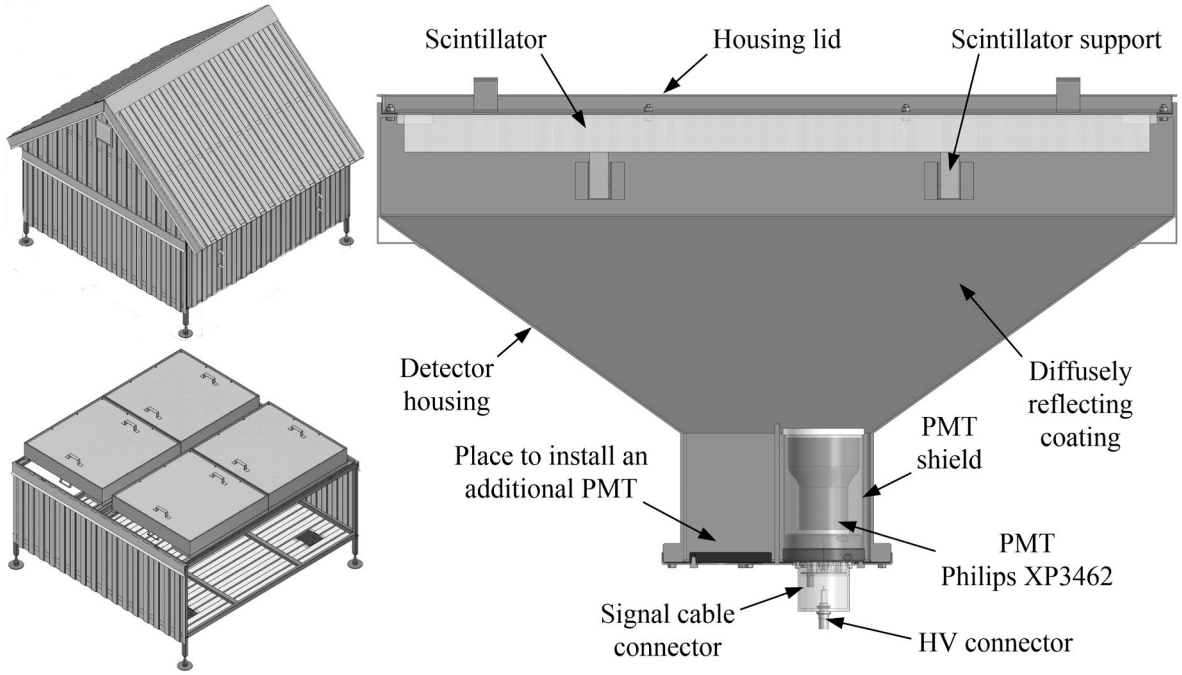

Fig. 2. The design of the NEVOD-EAS detector station: top left – detector station, bottom left – location of detectors inside the DS, right – scintillation detector.

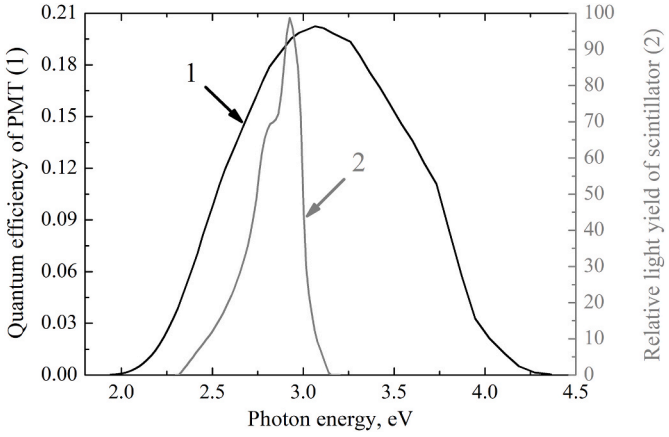

Fig. 3. –The quantum efficiency of PMT [21] and relative light yield of scintillator [19] as functions of photon energy.

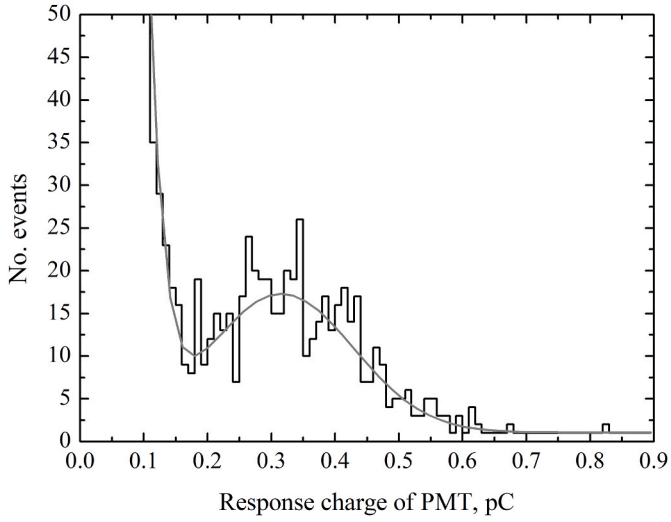

Fig. 4. Example of a charge spectrum of PMT responses to single-electron illumination (histogram – experimental distribution, curve – approximation by the sum of two normal distributions).

the non-uniformity of the detector response (dependence of the detector response on the place where the charged particle passes through the scintillator) obtained experimentally and as a result of the simulation.

An experimental study of the non-uniformity of light collection was carried out using the supermodule (SM) of the muon hodoscope URAGAN [22]. The URAGAN supermodule is a muon tracking detector with an area of 11.5 m^2. It consists of eight planes based on gas tubes operated in a limited streamer mode. With the supemodule single muon tracks are reconstructed with high spatial and angular accuracy (1 cm and 0.8°, respectively) in the zenith angle range from 0° to 80°. The hodoscope URAGAN is intended for muonography of the heliosphere, Earth's atmosphere and magnetosphere [23], but one of its supermodules is sometimes used to measure the non-uniformity of light collection of various detectors.

The facility to measure the non-uniformity of light collection (Fig. 5) consists of the SM URAGAN, on the top of which the under study detector is installed, a digital oscilloscope Tektronix MDO3034 recording signals from the under study detector, and two personal computers (PCs). One PC ensures operation of the SM, the second one receives data from the oscilloscope and combines them with the data of supermodule. When a charged particle passes through the SM, the supermodule generates a trigger for the oscilloscope. The oscilloscope transmits the digitized waveform of the recorded detector signal to the PC of the facility. At the same time, this computer receives information about the particle track coordinates and direction form the PC of the supermodule. For the analysis, we selected only events with single muons crossing the scintillator at zenith angles smaller than 15°. Near-vertical tracks are selected to ensure accurate determination of the coordinates and to ensure close energy deposit of muons in the scintillator.

Fig. 6 (left) shows the experimentally measured matrix of average charges of the detector responses to the passage of single muons. The matrix cell size is 1 × 1 cm^2. The statistical reliability of each cell is ~15 events. The coordinates of the cells in centimeters are plotted along the

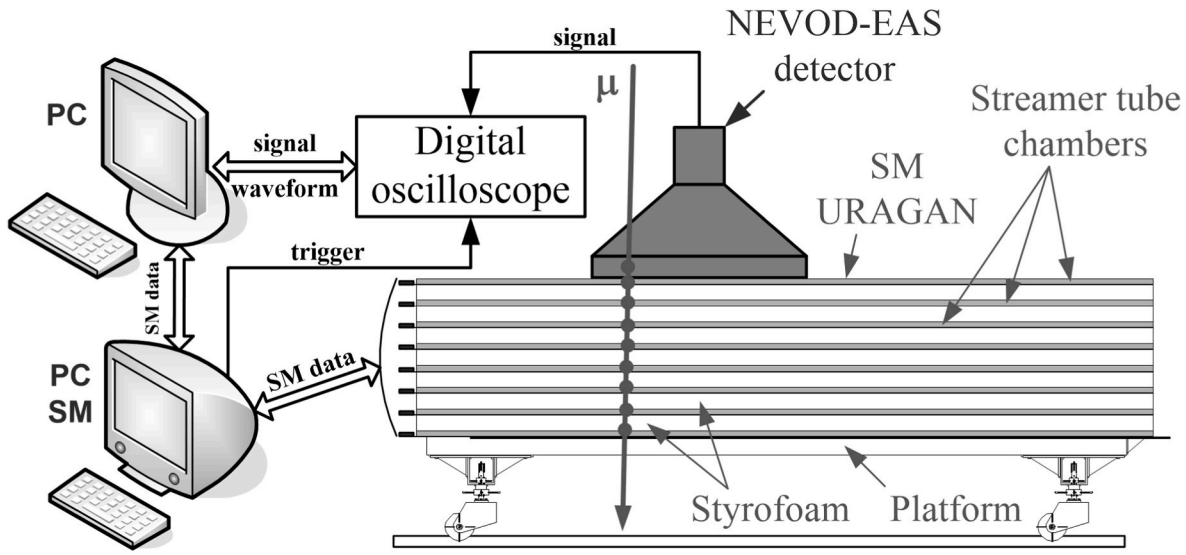

Fig. 5. Scheme of the facility for measuring light collection non-uniformity of detectors [17].

matrix axes. The top and side graphs show the variation of the detector response charge relative to the charge, averaged over the scintillator area, in two mutually perpendicular sections. The sections are marked on the matrices with dashed lines. As can be seen, the maximum light collection is observed from the area which in tests is located directly under the PMT (in the experiment it is located directly above the PMT). The observed shift of this area relative to the center of the detector is due to the non-central location of the PMT mounts in the housing due to the need to install an additional photodetector.

A similar matrix was obtained by simulating the detector response to single muons passing through different parts of the scintillator surface at zenith angles smaller than 15° (Fig. 6, right). The simulation of muons was carried out taking into account their spectrum which was calculated using the CORSIKA [24] (description is given in the next section).

As seen from Fig. 6, the shapes of the experimental and simulated matrices are in good agreement. In both cases, the light collection non-uniformity is defined as the ratio of the standard deviation calculated from the array of all cells to the average value. The experimental value of the light collection non-uniformity is 18.4 ± 0.1 %, while the simulated value is 18.2 ± 0.1 %. Thus, it can be concluded that the developed model gives a response close to the response of a real NEVOD-EAS scintillation detector, and can be used for its energy calibration.

5. Energy calibration of the detector station

During the operation of the NEVOD-EAS array, the monitoring is performed every 4 h. In the monitoring, the charge spectra of all 36 detector stations are measured in the self-triggering mode. In this mode, signals from detector stations are mainly due to the passage of single muons. To a lesser extent, the signals can be caused by the passage of hadrons, high-energy electrons and gammas. The typical most probable charge of the muon peak of the NEVOD-EAS detector stations is about 13 pC [15]. For the energy calibration of the DSs, it is necessary to determine the energy deposit corresponding to the peak value of the charge spectrum obtained in monitoring mode.

Using the developed model, we have simulated the DS response to single particles: muons, electrons, protons and gammas. When drawing the tracks of muons, protons and gammas, we used differential spectra for different values of the zenith angle [25] obtained by simulation with CORSIKA [24]. To simulate the energy of electrons and gamma-rays, we used a differential spectrum combining the results of CORSIKA simulations for kinetic energies above 100 MeV and those of calculation [26]

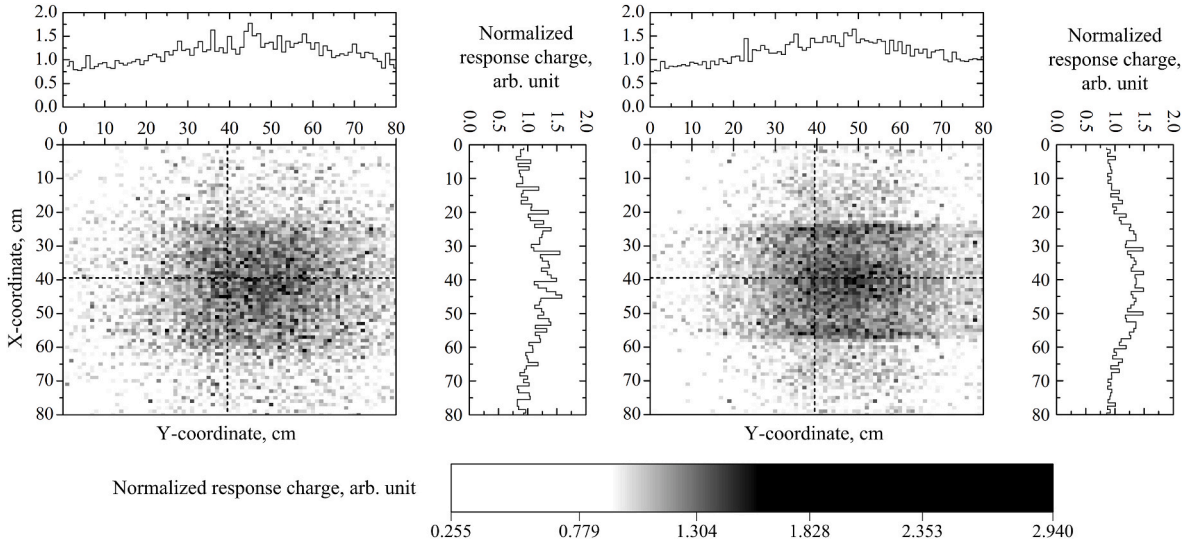

Fig. 6. Matrices of the normalized response charge of the NEVOD-EAS detector obtained experimentally (left) and by simulation (right).

for kinetic energies below 100 MeV. An example of the spectra of the abovementioned particles for the vertical direction is shown in Fig. 7.

Fig. 8 shows the distributions of the energy deposit of single particles inside the NEVOD-EAS detector station obtained by the simulation: for electrons, for muons, for gammas and summed for all types of particles. There are two peaks in the distribution. The left peak is due to the energy losses of electrons and gammas with energies of several MeV. The right one with the most probable value δE_{peak} of 11.5 MeV and the full width (FWHM) of 5.3 MeV is mainly contributed by the energy deposits of muons and electrons. At values greater than 8.6 MeV (0.75 of the most probable value δE_{peak}), the average energy deposit of muons is 14.8 MeV, and their contribution to the summed distribution is 71.6 %. The average energy deposit of electrons is 14.4 MeV with a contribution of 22.8 % to the summed distribution. Protons (1.9 %) and gammas (3.7 %) with average energy deposits of 34.9 and 17.8 MeV, respectively, represent a small contribution to the summed distribution. Due to the insignificance of its contributions, individual distribution for protons is not presented. The average energy deposit of all particles in DS $<\delta E>$ is 15.2 MeV.

Next, we have compared the charge spectrum of the DS responses obtained from simulated events with the experimental charge spectrum measured in self-triggering mode. To obtain agreement between simulation and experiment, the PMT gain in the model was multiplied by a scale factor of 0.386. The experimental and simulated spectra are shown in Fig. 9 as a histogram and a curve, respectively. The left peak in the experimental distribution is explained by the contribution of the natural radioactivity background and of the PMT dark noise. It is quite difficult to take these factors into account in simulation, so the left peak is absent in the spectrum of simulated DS responses. The right peak in the experimental distribution is due to the passage of cosmic ray particles. Its shape is well reproduced by the spectrum of simulated DS responses. The most probable response charge Q_{peak} is 13 pC, the full width at half maximum of the distribution $FWHM_Q$ is 9.1 pC.

It should be noted that the relative peak width of the charge spectrum ($FWHM_Q/Q_{peak} = 0.7$) is noticeably larger than the relative width of the energy deposit peak ($FWHM_{\delta E}/\delta E_{peak} = 0.46$). This is explained by additional fluctuations, which are introduced into the DS response by the light collection non-uniformity of the detector and by the Poisson fluctuations of the processes in the PMT. At a light collection non-uniformity of 18.1 %, the contribution to the relative peak width can be estimated as $\sim 2.35 \times 0.18 = 0.42$, where 2.35 is the relation between FWHM and sigma of the Gaussian distribution. In other words, the contribution of the light collection non-uniformity is comparable with energy deposit fluctuations. The contribution of Poisson fluctuations in the PMT can be estimated from the number of photoelectrons: at the most probable response of 13 pC the PMT detects ~42 photoelectrons. Thus, the contribution of Poisson fluctuations is $\sim 2.35/\sqrt{42} = 0.36$. The combination of energy deposit fluctuations, light collection non-uniformity and Poisson fluctuations in the PMT determines the relative width of the charge distribution peak ($0.46^2 + 0.42^2 + 0.36^2 \approx 0.7^2$).

The calibration coefficient, necessary for the reconstruction of experimental events, can be calculated as the ratio of the obtained values of δE_{peak} and Q_{peak} and is equal to 0.88 ± 0.04 MeV/pC.

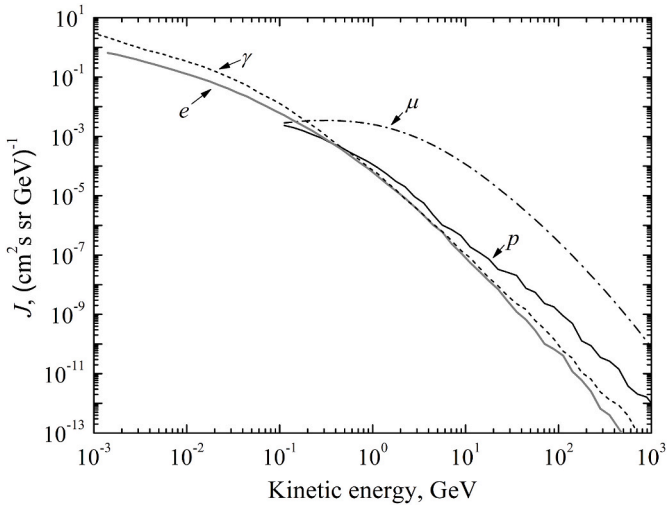

Fig. 7. The example of the energy spectra of particles used in simulation (muons, electrons, protons and gammas) for vertical direction.

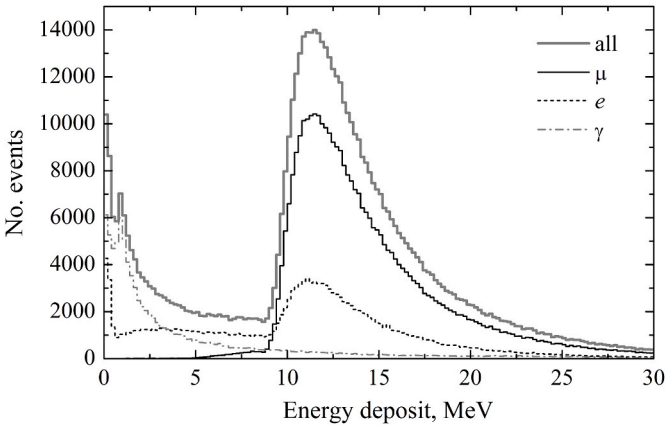

Fig. 8. Distributions of the energy deposit of single particles in the scintillator (results of simulation using the Geant4 software package).

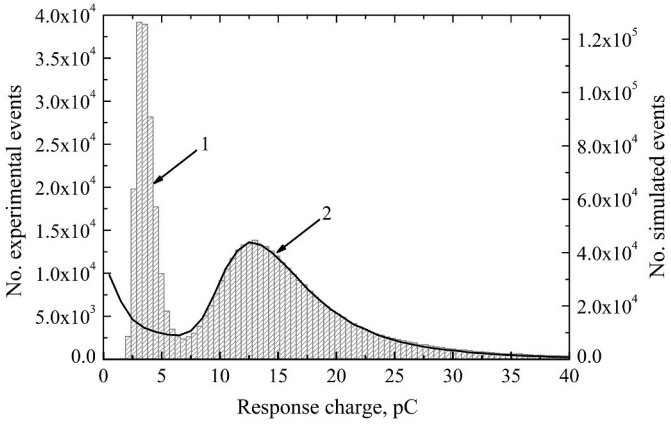

Fig. 9. Experimental (histogram "1") and simulated (curve "2") charge spectra of the responses of the NEVOD-EAS detector station obtained in self-triggering mode.

6. Response of scintillation detector to EAS electrons

When reconstructing the parameters of extensive air showers, it is assumed that the main contribution to the measured energy deposit is made by the electron-photon component.

To study the response of the scintillation detector to the EAS electron-photon component using the developed DS model we have simulated its response to electrons and gammas of fixed energies in the range from 10 to 100 MeV. Fig. 10 shows dependence of the average energy deposit of vertical electrons and gammas on their energies.

Gammas contribute to energy deposit through two processes: the Compton effect and the production of electron-positron pairs. Interactions of gammas can occur both in the scintillator itself and in the steel housing lid installed above the scintillation plate. According to the database [27], the cross sections of Compton effect in steel and

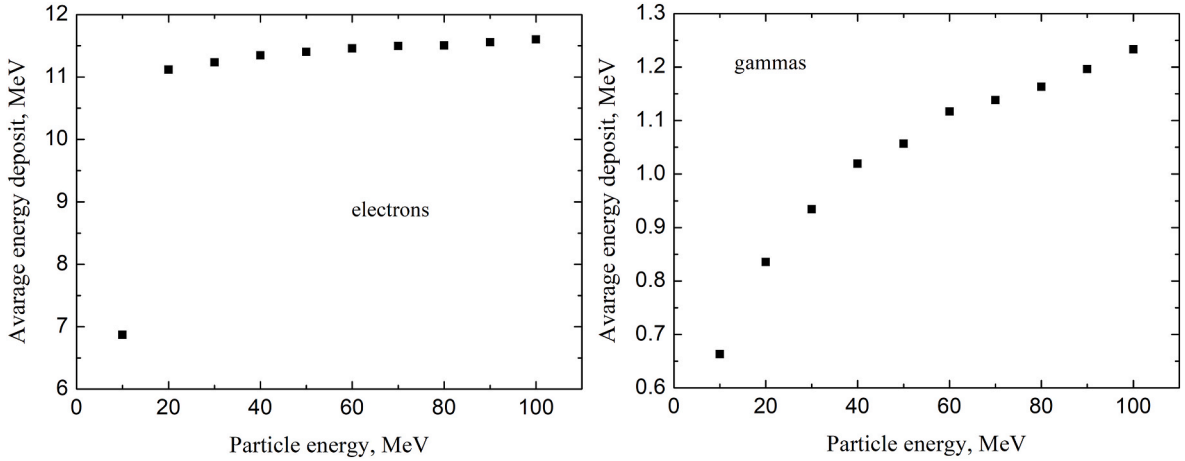

Fig. 10. The average energy deposit of vertical electrons (left) and gammas (right) in the detector station as a function of their energy obtained by simulation.

polystyrene are close to each other for gammas with energies from 10 to 100 MeV. At the same time the cross section of pair formation in steel is 3.5–3.8 times higher than in the scintillator. Taking into account the thicknesses of the steel lid (0.8 g/cm^2) and the scintillator (4.1 g/cm^2), one can obtain that the pair production in the lid and in the scintillator make almost the same contribution to the energy deposit of gammas. For gammas with energies less than 30 MeV, the cross section of Compton effect in polystyrene is higher than those for the pair formation. So in this energy range, the Compton effect in polystyrene causes up to 50 % of the energy deposit of gammas. It should be noted that, in this case, the Compton effect in the lid makes almost no contribution due to the small probability of interaction. The overall increase in the average energy deposit of gammas in the NEVOD-EAS detector is explained by the growth of the pair production cross section, which is 2.9 times for polystyrene and 2.6 times for steel in the energy range of gammas from 10 to 100 MeV.

As can be seen from the figure, the average energy deposit of particles increases with the growth of energy. As a rule, electrons with energy of 10 MeV lose part of their energy in the steel housing and then stop in the scintillator; therefore, their average energy losses significantly differ from the losses of more energetic electrons. At the critical electron energy (93.1 MeV for the NE102A scintillator) the average losses for electrons are about 11.5 MeV. Since the losses of the vertical minimum ionizing particle in the scintillation detector are 8.0 MeV, the energy deposit of electrons with critical energy is equivalent to the energy deposit of ~1.4 MIP. A weak increase in the average energy deposit of electrons with the energy is explained by the fact that the radiation length of the scintillation plate (41.3 cm) exceeds its thickness (4 cm) by an order of magnitude, and the bremsstrahlung gammas leave the scintillator without interaction.

We have also studied the response of the scintillation detector to electrons and gammas with energies simulated according to the spectrum of EAS particles. To do this, in CORSIKA using the models of hadronic interactions QGSJET–II–04 and FLUKA 2020.0.3, we have simulated extensive air showers originated by protons with energies of 10^{15}–10^{17} eV, distributed by a power-law energy spectrum with the exponent ($\gamma + 1$) of 2.7, and with zenith angles in the range from 0° to 30°. Using the simulation data, we have obtained the energy spectra (Fig. 11) of electrons and gammas of air-showers with a size greater than 10^5 electrons for two cases: for all EAS particles and for particles of EAS central part (within 100 m from the EAS axis); the threshold of kinetic energy for tracking secondary particles was 1 MeV. According to the review [1], the typical energies of electrons and gammas in air-showers are 40 MeV and 10 MeV, respectively. The mean logarithmic energies of particles in the obtained spectra are 24 MeV for electrons and 9 MeV for gammas for the first sample of particles (all EAS particles) and 30 MeV for electrons and 12 MeV for gammas for the second one, i.e. they are in a qualitative agreement with the above-mentioned review.

Using these spectra, we have simulated the response of the NEVOD-EAS detector station to electrons and gammas. Fig. 12 shows the distributions of simulated events by the energy deposits of EAS electrons and gammas in the detector station for two samples of particles.

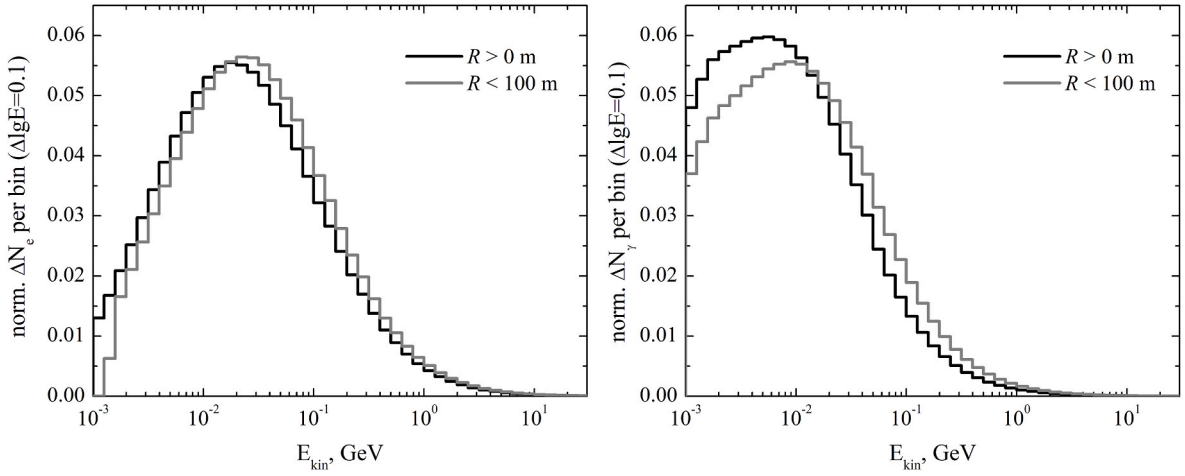

Fig. 11. The energy spectra of EAS electrons (left) and gammas (right) for two cases: for all EAS particles and for particles within 100 m from the EAS axis.

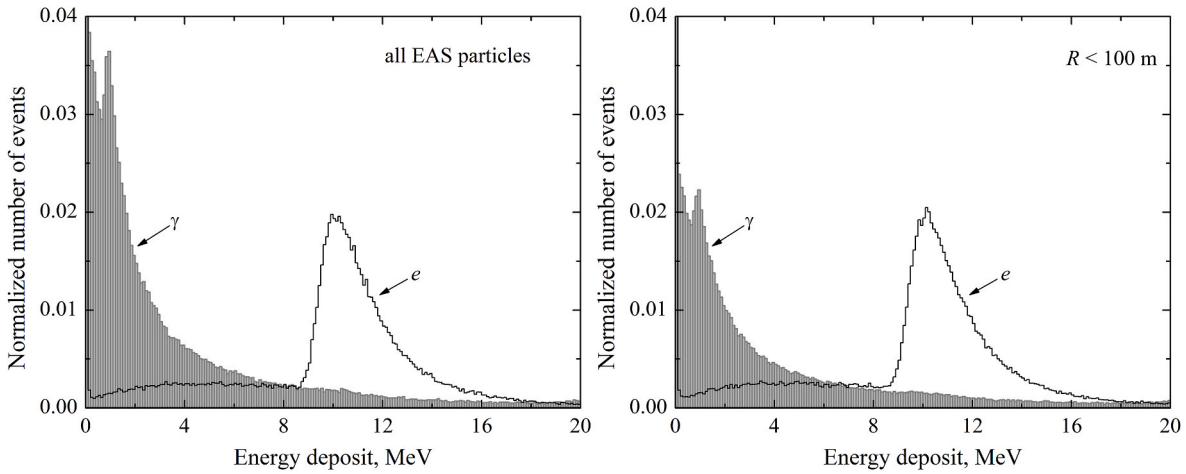

Fig. 12. The spectra of energy deposits of electrons and gammas in the detector station obtained by simulation for two samples of particles: all particles (left) and particles within 100 m from the EAS axis (right).

Most gammas pass through the scintillation detector without interaction. When simulating using the spectrum of all EAS gammas, the energy deposit is observed only in 15.8 % of events. When simulating using the spectrum of gammas of EAS central part, the energy deposit is observed in 14.8 % of events. In both cases, the spectra of energy deposits of gammas have peaks with the most probable value of 0.95 MeV. The average energy deposits are 0.64 and 0.7 MeV, correspondingly.

Some EAS electrons also do not produce energy deposit in the detector, because they stop in its steel lid. The energy deposit in the scintillator is provided by 81.1 % of all EAS electrons and 81.7 % of electrons from the EAS central part. In the spectra, the peaks with most probable values of 9.95 MeV for all EAS electrons and 10.15 MeV for electrons, arriving at a distance of less than 100 m from the axis, are observed. In both cases, the FWHM of these peaks are 2.5 MeV. The average energy deposit of electrons is 8.22 MeV for the first sample of particles and 8.26 MeV for the second one.

The average energy deposit of electrons from the EAS central part (8.26 MeV) is close to the value used for EAS parameters reconstruction in the EAS-TOP (8.2 MeV [2]) and KASCADE-Grande (8.5 MeV [4]) experiments, where these scintillation detectors were previously operated.

Thus, the obtained values of the average energy deposits of EAS electrons, as well as of the energy calibration coefficient, make it possible to estimate the number of particles that passed through each DS in an EAS event and, based on that, to reconstruct the air-shower size.

7. Estimation of the detector station timing resolution

The extensive air shower arrival direction is calculated on event-by-event basis, using the difference of the response times of the cluster detector stations. Therefore, the accuracy of EAS arrival direction reconstruction depends on the timing resolution of the DS.

To estimate the timing resolution of the detector station, we have carried out a test run of data taking at one of the NEVOD-EAS array clusters. The cluster configuration was changed as follows (see Fig. 13). One of four cluster DSs was disconnected from the recording system of the local post of preliminary data processing. Scintillation detectors of another station were divided into two substations A and B, consisting of

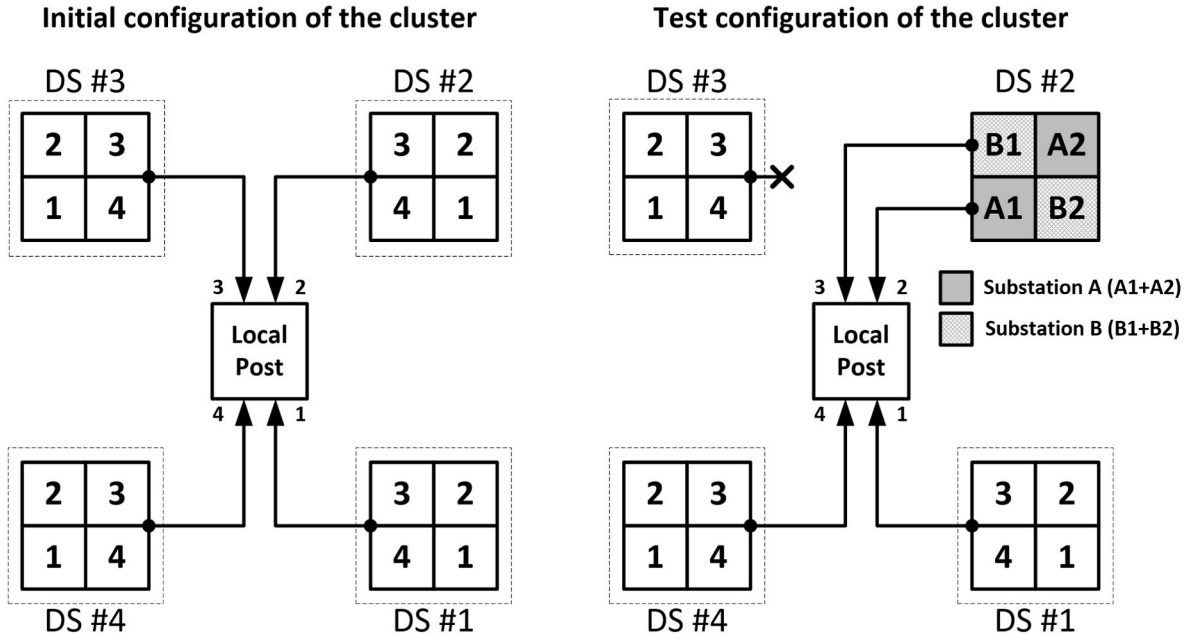

Fig. 13. Test configuration of a cluster for estimating timing resolution of the NEVOD-EAS detector station.

two detectors located on the diagonals of the DS. Substation A remained connected to the same channel of the cluster recording system as the original DS. Substation B was connected to the channel of the previously disconnected DS. In such configuration, when detecting EAS, both substations must respond to the passage of air-shower front almost simultaneously regardless of its the arrival direction. The duration of the test run was about 24 h. The coincidence of two full DSs and two substations was used as trigger condition. The detection threshold of the cluster measuring channels corresponded to ~0.75 of the muon peak most probable value. During the test run, 10519 events were detected.

Fig. 14 shows the distribution of events by the differences between the response times of substations A and B. The average value of the distribution is close to zero (0.01 ± 0.03 ns). That means that in all events the substations responded almost simultaneously. The FWHM is ~4.4 ns.

Since the distribution presents the difference between the response times of two substations, the timing resolution of one DS is $\sqrt{2}$ times less. Thus, the error of determination of the DS response time is ~3.1 ns, which corresponds to the size of the scintillation detector (about 1 m).

8. Accuracy of EAS arrival direction reconstruction

The accuracy of EAS arrival direction reconstruction was determined by comparing the results of reconstructions carried out according to the data of the NEVOD-EAS array and the muon tracking detector DECOR.

The muon tracking detector DECOR is located inside the building of the Experimental Complex NEVOD [12]. It consists of 8 vertical supermodules with a total area of 70 m^2 [28]. The supermodules have good spatial and angular resolution (~1 cm and ~1°) for muon tracks. The DECOR detector allows the detection of muon bundles in inclined EASs and the measurement of particle density of bundles [29]. Since muon bundles retain the primary particle direction with good accuracy, the EAS direction reconstructed by the muons can be compared with the direction obtained by the electron-photon component.

The NEVOD-EAS array and the muon tracking detector DECOR are connected to the global time synchronization system [12] of the Experimental Complex NEVOD, which ensures timestamping of events recorded by these facilities with accuracies of 10 and 25 ns, respectively.

Fig. 15 shows the distribution of events in the NEVOD-EAS and DECOR by the differences of timestamps. It is seen that on average, the DECOR detector is triggered 570 ns later than the NEVOD-EAS, and the vast majority of events falls within the range of ±100 ns from the average value of the distribution. The observed time shift and width of

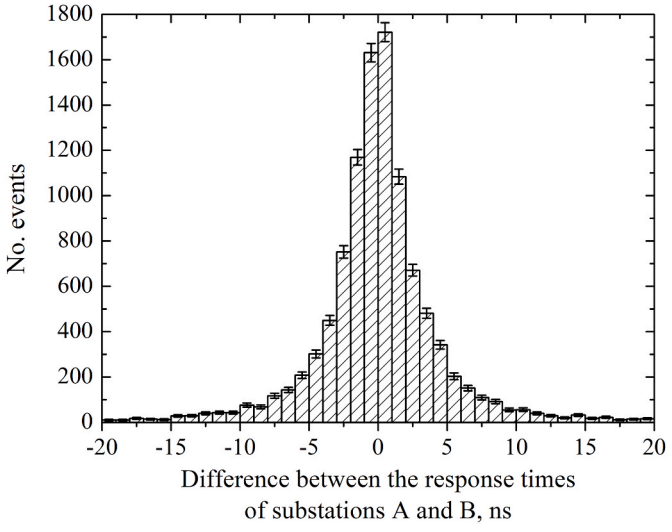

Fig. 14. Distribution of events by the differences between the response times of substations.

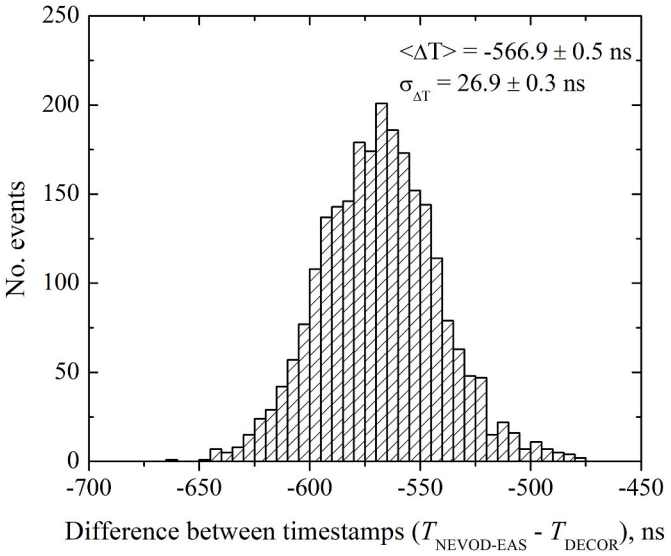

Fig. 15. Timestamp difference distribution of events in the NEVOD-EAS and DECOR.

distribution are due to the operation features of the DECOR trigger system in various classes of events. In further analysis, events in the NEVOD-EAS array and in the DECOR detector were considered as joint ones, if the difference in timestamps was in range from 470 to 670 ns.

For the joint analysis, from the data of the NEVOD-EAS array we selected events in which at least five clusters had been triggered. From the DECOR data, we selected events in which 3 or more muon tracks had been detected by at least 3 supermodules. We have analyzed a 70-day period of operation of the facilities and selected 2456 joint events with arrival direction zenith angles in the range from 10° to 60°. Due to the vertical arrangement of the supermodules, the acceptance of the muon tracking detector DECOR increases with the growth of zenith angle. Thus, 80 % of the selected joint events have zenith angles of arrival direction in the range from 20° to 45°.

When analyzing the NEVOD-EAS data, we used two methods to reconstruct the air-shower arrival direction. In the first method, the reconstruction of the direction was preliminary carried out according to the data of individual clusters, and the resulting EAS direction vector was determined as the average vector of all “cluster” directions. In the second, traditional method, we considered all detector stations of the NEVOD-EAS as elements of a single array, and the reconstruction of the air-shower arrival direction was carried out according to the data of all hit DSs. Taking into account the small size of the facility compared to the geometrical sizes of EASs, we used the approximation of a flat air-shower front in both methods.

To estimate the accuracy of EAS arrival direction reconstruction, for each of the selected events we determined the angular deviation between the muon bundle direction obtained with the DECOR and the air-shower direction reconstructed by the NEVOD-EAS data. The resulting distributions of joint events by the angular deviation are shown in Fig. 16. Large values of the angular deviation can be associated with the detection of small-sized showers or showers with axes falling on the periphery of the facility.

We have chosen the boundary, to the left of which fall 68.3 % of all events, as an estimate of the arrival direction reconstruction accuracy. When reconstructing according to the data of individual clusters, the accuracy is 5.9° ± 0.1°. Such accuracy is mainly determined by the temporal resolution of the DS (~3.1 ns), since for a typical cluster with dimensions of 15 × 15 m^2, the expected accuracy of arrival direction reconstruction is ~1/15 radian. In Ref. [15], using simulated events it was shown that such method for air-shower direction reconstruction provides accuracy better than 5° for primary particle energies above 1

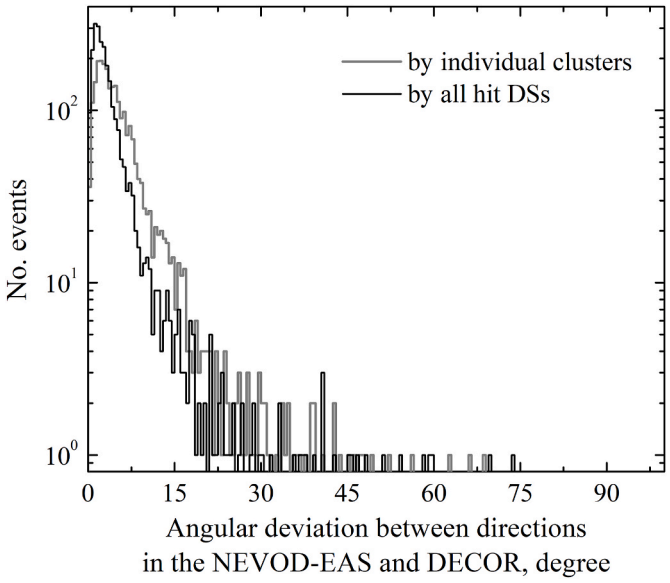

Fig. 16. Distribution of joint events by angular deviations of directions reconstructed according to the data of the DECOR detector and the NEVOD-EAS array.

PeV. Thus, the obtained experimental results are in good agreement with the simulation.

When reconstructing the direction according to the data of all hit DSs, the accuracy of cluster synchronization and the deviation of the EAS front shape from the plane becomes the determining factors. The reconstruction accuracy of this method improves up to $3.5^\circ \pm 0.1^\circ$.

9. Conclusion

For the energy calibration of the detector stations of the NEVOD-EAS air-shower array, a DS model has been developed using the software Geant4. The model has been verified using experimental data obtained in the study of the non-uniformity of light collection of the NEVOD-EAS scintillation detector carried out at the muon hodoscope URAGAN. A good agreement between the simulation and experimental results has been shown.

Simulating the DS response to single muons, electrons, protons, and gamma rays, we have shown that the most probable value of the charge spectrum peak (typical value is 13 pC), measured at all NEVOD-EAS stations in monitoring mode, corresponds to energy deposit of 11.5 MeV. Thus, the coefficient for converting the DS response charge into the energy deposit is 0.88 MeV/pC.

Also using the developed DS model, it has been determined that the typical energy deposit of EAS vertical electrons in a detector station is 8.26 MeV.

Comparing the EAS arrival directions reconstructed, in joined events, by the NEVOD-EAS and by the DECOR detectors, we have obtained that EAS arrival direction is measured by the air-shower array with a 3.5-degree accuracy.

Declaration of competing interest

The authors declare that they have no known competing financial interests or personal relationships that could have appeared to influence the work reported in this paper.

Data availability

Data will be made available on request.

Acknowledgments

The work was performed at the Unique Scientific Facility "Experimental Complex NEVOD" at the expense of the grant from the Russian Science Foundation No. 22-72-10010, https://rscf.ru/project/22-72-10010/.

The authors would also like to express gratitude to the KASCADE-Grande collaboration and the Institut für Astroteilchenphysik of the KIT for their material contribution to the maintenance and development of the NEVOD-EAS air shower array.

References

[1] P.K.F. Grieder, Extensive Air Showers: High Energy Phenomena and Astrophysical: a Tutorial, Reference Manual and Data Book, Springer, Berlin, London, 2010.
[2] M. Aglietta, B. Alessandro, P. Antonioli, F. Arneodo, L. Bergamasco, et al., UHE cosmic ray event reconstruction by the electromagnetic detector of EAS-TOP, Nucl. Instrum. Methods 336 (1–2) (1993) 310–321.
[3] T. Antoni, W.D. Apel, F. Badea, K. Bekk, A. Bercuci, et al., The cosmic-ray experiment KASCADE, Nucl. Instrum. Methods 513 (3) (2003) 490–510.
[4] W.D. Apel, J.C. Arteaga, A.F. Badea, K. Bekk, M. Bertaina, et al., The KASCADE-Grande experiment, Nucl. Instrum. Methods 620 (2–3) (2010) 202–216.
[5] X. Bertou, P.S. Allison, C. Bonifazi, P. Bauleo, C.M. Grunfeld, et al., Calibration of the surface array of the Pierre auger observatory, Nucl. Instrum. Methods 568 (2) (2006) 839–846.
[6] M. Amenomori, X.J. Bi, D. Chen, S.W. Cui, Danzengluobu, et al., The all-particle spectrum of primary cosmic rays in the wide energy range from 10^{14} to 10^{17} eV observed with the Tibet-III air-shower array, Astrophys. J. 678 (2008) 1165–1179.
[7] R. Abbasi, Y. Abdou, T. Abu-Zayyad, M. Ackermann, J. Adams, et al., All-particle cosmic ray energy spectrum measured with 26 IceTop stations, Astropart. Phys. 44 (2013) 40–58.
[8] Xin-Hua Ma, Yu-Jiang Bi, Zhen Cao, Ming-Jun Chen, Song-Zhan Chen, et al., Chapter 1 LHAASO instruments and detector technology, Chinese Phys. C 46 (2022), 035001.
[9] A. Aab, et al., Pierre auger collaboration, measurement of the cosmic-ray energy spectrum above 2.5×10^{18} eV using the Pierre auger observatory, Phys. Rev. D 102 (2020), 062005.
[10] P.A. Bezyazeekov, N.M. Budnev, O.A. Gress, A. Haungs, R. Hiller, et al., Measurement of cosmic-ray air showers with the Tunka radio extension (Tunka-Rex), Nucl. Instrum. Methods 802 (2015) 89–96.
[11] R. Abbasi, Y. Abdou, M. Ackermann, J. Adams, J.A. Aguilar, et al., IceTop: the surface component of IceCube, Nucl. Instrum. Methods 700 (2013) 188–220.
[12] I.I. Yashin, M.B. Amelchakov, I.I. Astapov, N.S. Barbashina, A.G. Bogdanov, et al., NEVOD – an experimental complex for multi-component investigations of cosmic rays and their interactions in the energy range $1–10^{10}$ GeV, J. Inst. Met. 16 (2021), T08014.
[13] A.A. Petrukhin, Muon puzzle in cosmic ray experiments and its possible solution, Nucl. Instrum. Methods 742 (2014) 228–231.
[14] H.P. Dembinski, J.C. Arteaga-Velázquez, L. Cazon, R. Conceição, J. Gonzalez, et al., Report on tests and measurements of hadronic interaction properties with air showers, Europ. Phys. J. Web Conf. 210 (2019), 02004.
[15] M.B. Amelchakov, N.S. Barbashina, A.G. Bogdanov, A. Chiavassa, D. M. Gromushkin, et al., The NEVOD-EAS air-shower array, Nucl. Instrum. Methods 1026 (2022), 166184.
[16] M. Aglietta, B. Alessandro, G. Badino, L. Bergamasco, C. Castagnoli, et al., The EAS-TOP array at Gran Sasso: results of the electromagnetic detector, Nucl. Phys. B Proc. Suppl. 16 (1990) 493–494.
[17] O.I. Likiy, N.V. Ampilogov, I.I. Astapov, N.S. Barbashina, N.N. Kamlev, et al., Investigating the characteristics of scintillation detectors for the NEVOD-EAS experiment, Instrum. Exp. Tech. 59 (2016) 781–788.
[18] S. Agostinelli, J. Allison, K. Amako, J. Apostolakis, H. Araujo, et al., Geant4 collaboration, Geant4 – a simulation toolkit, Nucl. Instrum. Methods 506 (3) (2003) 250–303.
[19] Saint-Gobain, Organic scintillation materials and assemblies. https://luxiumsolutions.com/files/816/download. (Accessed 19 May 2023).
[20] R.L. Workman, V.D. Burkert, V. Crede, E. Klempt, U. Thoma, et al., Particle data group, review of particle physics, Prog. Theor. Exp. Phys. (2022), 083C01.
[21] Photonis Group, Photomultiplier Tubes Catalogue, 2007. https://hallcweb.jlab.org/DocDB/0008/000809/001/PhotonisCatalog.pdf. (Accessed 19 May 2023).
[22] N.S. Barbashina, R.P. Kokoulin, K.G. Kompaniets, G. Mannocchi, A.A. Petrukhin, et al., The URAGAN wide-aperture large-area muon hodoscope, Instrum. Exp. Tech. 51 (2008) 180–186.
[23] N.S. Barbashina, A.A. Petrukhin, V.V. Shutenko, Method of muonography and prospects of its further development, Phys. Atom. Nucl. 84 (2021) 1182–1194.
[24] D. Heck, J. Knapp, J.N. Capdevielle, G. Schatz, T. Thouw, CORSIKA: a Monte Carlo code to simulate extensive air showers, Forschungszentrum, Karlsruhe, FZKA-6019 (1998).
[25] A.A. Kovylyaeva, A.N. Dmitrieva, N.V. Tolkacheva, E.I. Yakovleva, Calculations of temperature and barometric effects for cosmic ray flux on the Earth surface using the CORSIKA code, J. Phys. Conf. Ser. 409 (2013), 012128.
[26] R.R. Daniel, S.A. Stephens, Cosmic-ray-produced electrons and gamma rays in the atmosphere, Rev. Geophys. Space Phys. 12 (2) (1974) 233–258.

[27] Physical Measurement Laboratory, XCOM: Photon Cross Sections Database, NIST Standard Reference Database 8 (XGAM), 2010. https://www.nist.gov/pml/xcom-photon-cross-sections-database. (Accessed 19 May 2023).
[28] N.S. Barbashina, A.A. Ezubchenko, R.P. Kokoulin, K.G. Kompaniets, A. A. Konovalov, et al., A coordinate detector for studying horizontal fluxes of cosmic rays, Instrum. Exp. Tech. 43 (2000) 743–746.
[29] R.P. Kokoulin, N.S. Barbashina, A.G. Bogdanov, S.S. Khokhlov, V.A. Khomyakov, et al., Measuring the Cherenkov light yield from cosmic ray muon bundles in the water detector, Nucl. Instrum. Methods A 952 (2020), 161586.